HHS Public Access

Author manuscript

Cancer Prev Res (Phila). Author manuscript; available in PMC 2017 April 01.

Published in final edited form as:

Cancer Prev Res (Phila). 2016 April ; 9(4): 265–274. doi:10.1158/1940-6207.CAPR-15-0316.

WHOLE-GENOME SEQUENCING OF SALIVARY GLAND ADENOID CYSTIC CARCINOMA

Eleni M Rettig[1], **C Conover Talbot Jr**[2], **Mark Sausen**[3], **Sian Jones**[3], **Justin A Bishop**[4], **Laura D Wood**[4], **Collin Tokheim**[5], **Noushin Niknafs**[5], **Rachel Karchin**[5,6], **Elana J Fertig**[7], **Sarah J Wheelan**[6], **Luigi Marchionni**[6], **Michael Considine**[7], **Shizhang Ling**[1], **Carole Fakhry**[1,9], **Nickolas Papadopoulos**[8], **Kenneth W Kinzler**[8], **Bert Vogelstein**[8,*], **Patrick K Ha**[1,9,*], and **Nishant Agrawal**[1,8,10,*]

[1]Department of Otolaryngology-Head and Neck Surgery, Johns Hopkins University School of Medicine, Baltimore, MD, United States

[2]Institute for Basic Biomedical Sciences, Johns Hopkins University School of Medicine, Baltimore, MD, United States

[3]Personal Genome Diagnostics, Baltimore, MD, United States

[4]Department of Pathology, Johns Hopkins University School of Medicine, Baltimore, MD, United States

[5]Johns Hopkins Institute for Computational Medicine and Department of Biomedical Engineering, Johns Hopkins University, Baltimore, MD, United States

[6]Department of Oncology, John Hopkins University School of Medicine, Baltimore, MD, United States

[7]Department of Oncology Biostatistics & Bioinformatics, Johns Hopkins University School of Medicine, Baltimore, MD, United States

[8]Ludwig Center for Cancer Genetics and Therapeutics, Howard Hughes Medical Institute, and the Sidney Kimmel Comprehensive Cancer Center, Johns Hopkins University School of Medicine, Baltimore, MD, United States

[9]Milton J. Dance Jr. Head and Neck Cancer Center, Greater Baltimore Medical Center, Baltimore, MD, United States

[10]Head and Neck Surgical Oncology, The University of Chicago Medicine, Chicago, IL, United States

[*]NA, PH and BV are co-corresponding authors. Correspondence should be addressed to: Nishant Agrawalm The University of Chicago Medicine, Head and Neck Surgical Oncologym 5841 S. Maryland Ave, Rm E-102, MC1035, Chicago IL 60637m Phone: 773-702-6143, Fax: 773-702-6809m nagrawal@jhmi.edu, Patrick K Ha, Koch Cancer Research Building II, Room 5M06, 1550 Orleans St., Baltimore MD 21231, Phone: 4105028210, Fax: 410-955-6526, pha1@jhmi.edu, Bert Vogelstein, Cancer Research Building I, Room 589, 1650 Orleans St., Baltimore MD 21231, Phone: 410-955-8878, Fax: 410-955-0584, vogelbe@jhmi.edu.

CONFLICTS OF INTEREST: Under agreements between the Johns Hopkins University, Genzyme, Sysmex-Inostics, Qiagen, Invitrogen and Personal Genome Diagnostics, NP, BV, and KWK are entitled to a share of the royalties received by the University on sales of products related to genes and technologies described in this manuscript. NP, BV and KWK are co-founders of Inostics and Personal Genome Diagnostics, are members of their Scientific Advisory Boards, and own Personal Genome Diagnostics stock, which is subject to certain restrictions under Johns Hopkins University policy. The terms of these arrangements are managed by the Johns Hopkins University in accordance with its conflict-of-interest policies.

Abstract

Adenoid cystic carcinomas (ACCs) of the salivary glands are challenging to understand, treat, and cure. To better understand the genetic alterations underlying the pathogenesis of these tumors, we performed comprehensive genome analyses of 25 fresh-frozen tumors, including whole genome sequencing, expression and pathway analyses. In addition to the well-described *MYB-NFIB* fusion which was found in 11 tumors (44%), we observed five different rearrangements involving the *NFIB* transcription factor gene in seven tumors (28%). Taken together, *NFIB* translocations occurred in 15 of 25 samples (60%, 95%CI=41–77%). In addition, mRNA expression analysis of 17 tumors revealed overexpression of *NFIB* in ACC tumors compared with normal tissues (p=0.002). There was no difference in *NFIB* mRNA expression in tumors with *NFIB* fusions compared to those without. We also report somatic mutations of genes involved in the axonal guidance and Rho family signaling pathways. Finally, we confirm previously described alterations in genes related to chromatin regulation and Notch signaling. Our findings suggest a separate role for *NFIB* in ACC oncogenesis and highlight important signaling pathways for future functional characterization and potential therapeutic targeting.

Keywords

Adenoid cystic carcinoma; salivary gland neoplasms; gene fusion; genome; NFI transcription factors

INTRODUCTION

Adenoid cystic carcinomas (ACCs) of the salivary glands are often indolent but can aggressively invade local structures and metastasize to distant sites many years after initial treatment.(1) ACC frequently spreads to nearby nerves, a process termed perineural invasion (PNI), which portends poor prognosis and higher likelihood of local recurrence.(2, 3) There are at present no reliable chemotherapeutic options for long-term disease control.

Recently, molecular and whole-exome sequencing studies have begun to shed light on the genetic underpinnings of this relatively rare disease.(4–7) A t(6;9)(q22–23;p23–24) chromosomal translocation resulting in fusion of the *MYB* and *NFIB* genes has been described in 29–86% of cases.(4, 5, 8–11) Whether the *MYB* oncogene or the transcription factor encoded by *NFIB* is responsible for the selective advantage afforded by these translocations is unknown. Frequent alteration of genes involved in chromatin regulation, Notch signaling and several other pathways have also been reported.(5–7) Whole-genome sequencing, which is capable of revealing chromosomal rearrangements not detectable by traditional cytogenetic techniques, has been applied to a limited number of tumors.(5, 12)

We performed whole-genome sequencing of 25 fresh-frozen surgically resected ACC tumors, and mRNA expression analysis of a subset of these tumors, to better understand the genetic alterations that drive ACC pathogenesis. We found novel rearrangements involving *NFIB* and show that *NFIB* is translocated in the majority (15 of 25, 60%) of tumors. *NFIB* mRNA was also overexpressed in ACCs compared with normal tissues. We also noted frequent disruption of axonal guidance and Rho family signaling pathways. Our findings

suggest a critical role for *NFIB* in ACC oncogenesis, and identify important signaling pathways for functional characterization and potential therapeutic targeting in the future.

Materials and methods

Sample preparation

Fresh-frozen surgically resected tumor and matched blood/normal tissue were obtained from patients under an Institutional Review Board protocol at the Johns Hopkins Hospital and from the Salivary Gland Tumor Biorepository. Informed consent was obtained from each patient. Tumor tissue was analyzed by frozen section histology to estimate neoplastic cellularity. In order to enrich the samples for neoplastic cells, normal tissue was removed from the samples using macro-dissection based on the frozen section histology. An estimated average of at least 60% neoplastic cellularity was obtained. DNA and RNA were purified using AllPrep (Qiagen, cat# 80204).

DNA sequencing

Whole-genome sequencing was performed in tumors from 25 patients. Tumor samples were carefully selected or dissected in order to achieve a neoplastic cellularity of >60%. DNA was purified from these tumors and from matched non-neoplastic tissue, and used to generate libraries suitable for massively parallel sequencing.

Sample library construction, next generation sequencing, and bioinformatic analyses of tumor and normal samples were performed at Personal Genome Diagnostics (Baltimore, MD). In brief, genomic DNA from tumor and normal samples were fragmented and used for Illumina TruSeq library construction (Illumina, San Diego, CA). Paired-end sequencing, resulting in 100 bases from each end of the fragments, was performed using a HiSeq 2000 Genome Analyzer (Illumina, San Diego, CA).

Somatic mutations were identified using VariantDx custom software for identifying mutations in matched tumor and normal samples. Prior to mutation calling, primary processing of sequence data for both tumor and normal samples were performed using Illumina CASAVA software (v1.8), including masking of adapter sequences. Sequence reads were aligned against the human reference genome (version hg19) using ELAND with additional realignment of select regions. Candidate somatic mutations, consisting of point mutations and small (<50bp) insertions and deletions were then identified using VariantDx across the exonic regions. VariantDx examines sequence alignments of tumor samples against a matched normal while applying filters to exclude alignment and sequencing artifacts. In brief, an alignment filter was applied to exclude quality failed reads, unpaired reads, and poorly mapped reads in the tumor. A base quality filter was applied to limit inclusion of bases with reported Phred quality scores >30 for the tumor and >20 for the normal.(13) A mutation in the tumor was identified as a candidate somatic mutation only when (i) distinct paired reads contained the mutation in the tumor; (ii) the number of distinct paired reads containing a particular mutation in the tumor was at least 2% of the total distinct read pairs for targeted analyses and 10% of read pairs for exome; (iii) the mismatched base was not present in >1% of the reads in the matched normal sample as well

as not present in a custom database of common germline variants derived from dbSNP; and (iv) the position was covered in both the tumor and normal. Mutations arising from misplaced genome alignments, including paralogous sequences, were identified and excluded by searching the reference genome. Candidate somatic mutations were further filtered based on gene annotation to identify those occurring in protein coding regions. Functional consequences were predicted using snpEff and a custom database of CCDS, RefSeq and Ensembl annotations using the latest transcript versions available on hg19 from UCSC.(14) Predictions were ordered to prefer transcripts with canonical start and stop codons and CCDS or Refseq transcripts over Ensembl when available. Finally mutations were filtered to exclude intronic and silent changes, while retaining mutations resulting in missense mutations, nonsense mutations, frameshifts, or splice site alterations. A manual visual inspection step was used to further remove artifactual changes. We have previously optimized our sequencing and bioinformatics approaches so that specificity of mutations is extremely high. This has been extensively validated by not only Sanger Sequencing but also by NGS at high depth. A minimum of 95% of the mutations identified using these approaches are bone fide.(15, 16)

Copy number alterations were identified by comparing normalized average per-base coverage for a particular gene in a tumor sample to the normalized average per-base coverage in a matched normal sample for that patient.(17) Focal amplifications (≥3-fold or six copies) and homozygous deletions were reported. Genomic rearrangements were identified through an analysis of discordantly mapping paired-end reads. The discordantly mapping paired-end reads were grouped into 1kb bins when at least 5 distinct tag pairs (with distinct start sites) spanned the same two 1kb bins, and further annotated based on the approximate breakpoint.(18) Genomic sequencing data deposition into a publicly available database is in process.

Randomization-based statistical test for proportion of truncating mutations

We performed a randomization-based statistical test of increased proportion of truncating mutations (S) out of total non-silent mutations (N) for genes involved in chromatin regulation, controlling for the effect of gene sequence and mutational context. For each gene *i,* our test statistic was

$$T_i = \frac{\#\{t : t \in S\}}{|N|} \quad where\, S \subset N$$

Truncating mutations were defined as any nonsense, conserved di-nucleotide splice site mutations or out-of-frame insertions/deletions (frameshift). Monte Carlo simulations were performed to approximate the null probability distribution of the test statistic T_i. Each Monte Carlo sample was generated by moving every observed non-silent single base substitution (SBS) mutation to uniformly sampled nucleotide positions within the same gene, with matched single nucleotide mutational context (*e.g.,* if a C->T was observed, the mutation had to be moved to a C reference position). However, the mutation consequence type of the C->T might change. For example, a SBS that generated a missense mutation

might generate a nonsense mutation in its new position. Because frameshift mutations do not change consequence when moved to a different position, in the Monte Carlo sample, they were retained with probability equal to the observed proportion of frameshift mutations out of all mutations (maximum likelihood estimate), otherwise they were changed to a non-truncating mutation. After each iteration of this sampling procedure, the number of mutations in a gene is always the same, but the mutation consequence of each mutation may change. Thus, the test statistic for the gene will change values at each iteration, and repeated iterations yield a null distribution of test statistics to estimate the p-value of the gene's observed test statistic. For the gene group analysis, our test statistic was

$$T_c = \frac{\sum_{i \in c} \#\{t : t \in S_i\}}{\sum_{i \in c} |N_i|}$$

and it was computed both for the observed and simulated mutations. A one-tailed empiricial p-value was calculated as the fraction of Monte Carlo samples in which the observed value of the test statistic was equal to or higher than the simulated value. Increasing the number of iterations of Monte Carlo sampling increases the precision of the p-value; 10,000,000 iterations were chosen to achieve adequate precision.

mRNA expression

Strand-specific sequencing libraries were prepared using the TruSeq Stranded Total RNA library kit (Illumina). Barcoded libraries were quality-controlled using the Kappa PCR kit and pooled in equimolar ratios for subsequent cluster generation and sequencing on an Illumina HiSeq 2000 instrument to yield >50,000,000 paired end 100 x 100 bp tags for each sample. Paired-end reads were then mapped to the human genome (build hg19) and expression levels of all known gene isoforms annotated in RefSeq, Ensembl, and UCSC gene annotations were derived using the RSEM package,(19) which uses an expectation maximization algorithm to derive the abundance of each gene isoform after taking into account the read mapping uncertainty with a statistical model. TopHat-Fusion was used to identify fusion transcripts from the RNA sequencing data.(20).

RSEM expected counts for gene were upper quartile normalized perl scripts from the TCGA RNA-seq V2 normalization pipeline.(22) Each gene was further normalized to a maximum value of 1 for visualization in a heatmap. Upper quartile normalized read counts were voom transformed for differential expression statistics.(23) All genes with overall log fold change greater than 0.25 were compared with empirical Bayes moderated t-statistics with equal variance implemented in the R/Bioconductor package LIMMA version 3.26.0.(24) P-values reported are Benjamini-Hotchberg corrected among the subset of seven genes in *NFIB* fusions and retained for differential expression analysis. mRNA expression data deposition into a publicly available database is in process.

Pathway analyses

Pathways analysis was performed on the DNA sequencing analysis results to identify biological pathways that are likely to be altered by the somatic mutations alone, and then by

both somatic mutations and chromosomal rearrangements observed in the 25 ACC samples analyzed, using Ingenuity Pathway Analysis (IPA) Build: 321501M (QIAGEN Redwood City). Two gene sets (mutations and mutations-plus-rearrangements) were separately uploaded to IPA and compared to their gene Knowledgebase to determine the known canonical pathways that contained the affected genes. The statistical significance of each pathway was reported as a p-value, determined using the right-tailed Fisher Exact Test, representing the likelihood that the given pathway was chosen by chance. Figures are provided for selected pathways, wherein the affected gene symbols are color-coded.

Results

Sequence mutations

Whole-genome sequencing was performed on 25 samples as described in the Methods section (Table S1 and Methods). The average coverage of each base in tumors was 51.7-fold overall (65.2-fold for tumors and 38.1-fold for matched non-neoplastic tissues), and 98.2% of targeted bases were represented by at least 10 reads (Table S1). We identified 396 somatic mutations (point mutations and small indels) in 372 genes among the 25 tumors. The range of mutations per tumor was 2 to 36, with a median of 14 (Table 1 and Table S2). Somatic mutations were identified in more than one tumor in 21 different genes. *NOTCH1* was the most frequently altered gene, with four mutations in three tumors including two substitutions (one nonsense and one non-synonymous), one frame-shift and one in-frame deletion. A non-synonymous substitution was also found in *NOTCH2*. Other genes found to have multiple mutations are recorded in Table 2.

Consistent with previous findings, several genes with well-known roles in chromatin regulation were mutated in multiple tumors: *MLL2*, *MLL3*, *EP300, SMARCA2, SMARCC1* and *KDM6A* (Table 1 and Table S2). The proportion of truncating mutations (nonsense codons, splice site alterations, or out-of-frame insertions and deletions) out of the total number of non-silent mutations in these genes was high (6 out of 11), significantly greater than expected by chance ($p=3.8 \times 10^{-6}$, randomization-based test). Furthermore, *MLL2* and *EP300* when considered individually had a significantly higher proportion of truncating mutations than expected by chance (p=0.008 for *MLL2* and p=0.01 for *EP300*). This finding is consistent with the hypothesis that several of these genes played an important role in the cancers in which they occurred.

Copy number variation

We identified 41 copy number variations (CNVs) in 12 of the 25 tumors sequenced, with a range of 0 to 9 CNVs per tumor (Table 1, Table S3). The most common CNVs included amplification of genes on 7p14.1 (five tumors) and 14q11.2 (four tumors). Both cytobands contain T-cell receptor genes. Several deletions of 10q26.3, containing DUX4 and DUX4L (DUX4-like) homeobox genes, were also observed (in three tumors).

Rearrangements

We observed a total of 253 chromosomal rearrangements in the 25 tumors (median 7 per tumor, range 0–42 rearrangements per tumor), including 118 interchromosomal (median 3

per tumor) and 135 intrachromosomal (median 3 per tumor) rearrangements (Tables 1 and S4, Figures 1 and S1). Chromosomal breakpoints were concentrated in several regions of the genome, particularly chromosome 6q (144 of 506 breakpoints, 28%) and 9p (71 breakpoints, 14%) (Figure 1).

ACCs have been shown to harbor t(6;9)(q23.3;p22.3) translocations resulting in *MYB-NFIB* fusion gene products.(4, 9, 11) We identified this translocation in 11 of 25 tumors (44%, 95%CI=27–63%); Table 1). We also identified five gene fusions involving *NFIB* that did not involve *MYB*, four of which are previously undescribed. These included t(6;9)(q23.3;p22.3) fusions involving *MAP3K5-NFIB* and t(8;9)(q13.1;p22.3) fusions involving *MYBL1-NFIB* in two tumors each (Table 1, Figure 2). *NFIB* also recombined with three other genes on chromosome 6q, *RPS6KA2, MYO6* and *RIMS1*. In contrast, *MYB* recombined with only one gene other than *NFIB* (Table S4). Overall, *NFIB* translocations occurred in 15 of 25 tumors (60%, 95%CI=41–77%). Three tumors with novel *NFIB* fusions also harbored *MYB-NFIB* fusions. The *NFIB* breakpoint locations for both *MYB-NFIB* and other *NFIB* fusions were heterogenous (Table S5).

The most frequent intrachromosomal rearrangements resulted in deletions (N=67 of 135 intrachromosomal rearrangements, 50%), with inversions (N=47, 35%) and duplications (N=21, 16%) less common (Table S4). The median size of intrachromosomally rearranged segments was 4,074 kb (range, 2–137,666 kb; IQR 167–29,034 kb). *NFIB* was involved in intrachromosomal rearrangements in three tumors (two deletions and one inversion), including one tumor (HN 324) that did not also have an *NFIB* translocation.

RNA sequencing fusion analysis and differential mRNA expression

To compare chromosomal rearrangements with mRNA fusion transcript expression, mRNA expression was assessed in the 17 tumors for which freshly frozen tumor tissue was available (see Methods). Two of the six tumors evaluated with non-*MYB NFIB* rearrangements expressed corresponding mRNA transcripts (*RIMS1-NFIB* and *MYBL1-NFIB;* Table 1). Of the nine tumors with *MYB-NFIB* rearrangement and available RNA, all were found to have *MYB-NFIB* mRNA transcripts. One additional tumor that did not have a *MYB-NFIB* rearrangement detected on whole-genome sequencing was found to have *MYB-NFIB* transcript expression (tumor HN 335 PT).

Differential expression of the genes in involved in *NFIB* fusions was also assessed. *NFIB* was overexpressed in tumors relative to normal tissues (p=0.002; Figure 3). *NFIB* expression was not significantly different in tumors with *NFIB* fusion genes compared to those without *NFIB* fusion genes (p=0.91).

MYB expression was also significantly higher in tumors than in normal samples (p<0.001). *MYB* was more highly expressed in tumors with *MYB-NFIB* fusion genes when compared to those without (p<0.001). The only two tumors that did not express *MYB* were those with *MYBL1-NFIB* fusion genes (HN 333 PT and HN 320 PT). These two tumors had significantly lower *MYB* expression compared with the other tumors (p<0.001), but had higher *MYBL1* expression than other tumors (p=0.07), although this latter difference was not statistically significant.

Genes other than *MYB* that were involved in *NFIB* fusions, including *MYO6, MAP3K5, RPS6KA2, RIMS1,* and *MYBL1*, did not have significantly different levels of expression in tumors compared with normal tissues (p>0.13 for all).

Pathway analyses

Ingenuity Pathway Analysis (IPA) software was used to identify biological pathways that might be altered by the somatic mutations observed in the 25 ACC samples. Interestingly, IPA revealed significant involvement of the Rho family GTPase signaling pathway, with 11 (44%, 95%CI=27–63%) tumors containing somatic mutations in one or more members of this pathway ($p=3.9x10^{-6}$), including *RHOA* (two tumors), *CDH2, CDH13, ARHGEF3, ARHGEF5, ARHGEF18, ACTB* and others (Figure 4). The axon guidance signaling pathway was also highly disrupted (14 tumors [56%, 95%CI=37–73%], $p=8.3x10^{-5}$), with mutations in *PLXNB1* (two tumors) *PRKD1* (two tumors*), SLIT1, PLXNA1, SRGAP2, SRGAP3, ADAM2, ADAMTS5, ADAMTS13, SEMA3G* (one tumor each)*,* and others (Figure S2).

IPA was also performed for all genes affected by any chromosomal rearrangement and/or somatic mutation, and identified disruptions of pathways involved in a variety of complex cellular processes that have previously been implicated in ACC, corroborating previous reports and validating our findings. These include protein kinase A (PKA) signaling (21 tumors), FGF signaling (15 tumors), Wnt/β-catenin signaling (13 tumors), PI3K/AKT signaling (13 tumors), and Notch signaling (9 tumors).(5–7, 25)

Discussion

Our whole genome sequencing data and analysis reveal previously unreported *NFIB* rearrangements and *NFIB* overexpression in ACC tumors, as well as genetic alterations of the Rho family signaling pathway. We also corroborate previous reports of alterations in axonal guidance signaling, chromatin regulation, *NOTCH1/2* somatic mutations, and involvement of key signaling pathways.

Our finding that *NFIB* rearrangements occur independently of *MYB* and are present in the majority of tumors, and that *NFIB* is significantly overexpressed in ACCs in comparison with normal tissues regardless of *NFIB* fusion status, suggests that *NFIB* may have a role in ACC oncogenesis independent of *MYB. MYB* is a transcription factor involved in proliferation, survival and differentiation, with well-known oncogenic capabilities.(26) Although *MYB* is overexpressed in 80% of ACCs, and is often, but not always, associated with the *MYB-NFIB* fusion, *MYB* overexpression does not appear to be a necessary step in the development of ACC.(6, 10, 11, 27) *NFIB* is a member of the nuclear factor I transcription family reported to be involved in rearrangements in other tumor types, although the significance of these rearrangements has not been well described.(28, 29) *NFIB* recombined with several genes in our cohort other than *MYB*, including two cases each with *MYBL1*, a transcriptional activator in the MYB family that has been implicated in pediatric low-grade gliomas(30) and a recently described fusion partner with *NFIB* in a subset of ACCs.(12, 31) Notably, the two tumors with *MYBL1-NFIB* fusions uniquely did not express *MYB* at all, consistent with reports of a mutually exclusive relationship between *MYB* and

MYBL1 alterations in ACC.(12, 31) The significance of the other *NFIB* fusion partners is unclear. Although we found recurrent fusions of *NFIB* with *MAP3K5* (also known as apoptosis signal-regulating kinase I, *ASK1*), a serine/threonine protein kinase with critical regulatory functions in the apoptotic pathway and reported roles in tumorigenesis,(32) the other three fusions occurred in only one tumor each; few were confirmed on mRNA expression analysis. None of these genes were identified in other recent reports of novel *NFIB* fusion partners in ACC.(5, 12) Interestingly, three of the 25 tumors in our study, and one of the five reported by Ho et al., contained *NFIB* fusions both with *MYB* and with a different gene.

The overexpression of the *NFIB* mRNA in ACC has not been previously reported to our knowledge. This did not appear related to the presence of *NFIB* fusions, implicating alternative mechanisms of *NFIB* dysregulation. *NFIB* is reported to behave as an oncogene in small cell lung cancer(33) and is overexpressed in estrogen receptor-negative breast cancer.(34) It is conceivable, therefore, that there is a role for *NFIB* overexpression in ACC oncogenesis. Taken together with the high prevalence of *NFIB* fusion genes, this constellation of findings suggest that *NFIB* may be contribute more significantly to ACC biology than has been previously appreciated. Further studies are necessary to evaluate the functional importance and potential therapeutic implications of *NFIB* alterations in ACC. (5, 12)

The Rho signaling pathway was significantly affected by somatic mutations in our cohort, and this has not been previously reported in ACC. The Rho GTPase family, including the Rho and Rac subfamilies, is involved in many aspects of carcinogenesis.(35) In particular, Rho signaling is a major regulator of motility, cytoskeleton structure, and adhesion in cancer cells, facilitating the tumor cell plasticity that allows for adaptation to and invasion of diverse tumor microenvironments.(36, 37) Rho protein expression and activity is frequently observed in human malignancies. (38) Although mutations of Rho GTPase proteins are rare, (35, 36, 39) a recurrent *RHOA* somatic mutation was recently identified in angioimmunoblastic T cell lymphoma. Interestingly, we found two different mutations in *RHOA* in two of the 25 ACC tumors analyzed in this study, and pathway analysis revealed significant disruption of the Rho pathway overall. This suggests a potential role for Rho signaling in ACC but additional functional and genomic work is required to solidify this conjecture.

The known predilection of ACC for perineural invasion, and the association of PNI with disease recurrence,(2, 3) adds importance to our finding that the axonal guidance signaling pathway is significantly altered in ACC. Somatic mutations of genes involved in axonal guidance signaling (including *NTNG1, SEMA3G,* and *SEMA5A*) were also previously noted by Ho *et al*,(5) and an identical *SEMA3G* non-synonymous substitution (474S>P) was observed in our cohort. Interestingly, significant disruptions of axonal guidance signaling pathways have also been noted in pancreatic adenocarcinoma, another malignancy characterized by frequent PNI that portends poor prognosis.(40, 41)

Our findings also confirmed several observations made in ACC exome sequencing studies. Somatic mutation of *NOTCH1, NOTCH2* and other Notch pathway molecules have been

previously reported in ACC,(5–7) and indeed *NOTCH1* was the most commonly disrupted gene in our cohort (12% of tumors). Notch signaling has pleiotropic context-dependent effects on cell differentiation, survival and growth, and is disrupted in many human malignancies.(42, 43) *NOTCH1* alterations can result in either tumor suppression or oncogenesis, depending on the tumor type.(44–46) Additional characterization of Notch signaling alterations in ACC is indicated, particularly because Notch signaling is a potentially targetable pathway.(42) Our findings also corroborate a high prevalence of somatic mutations in genes related to chromatin remodeling, including *MLL2, MLL3,* and *EP300,* among others. The finding that chromatin regulators are consistently altered in ACC supports an important role for epigenetic regulation of gene expression in ACC oncogenesis. (5, 6)

We observed recurrent amplifications of two loci containing T-cell receptor genes, however these findings should be interpreted with caution as they may be an artifact of T-cell receptor gene rearrangement.(47)

Our increasing understanding of ACC's molecular characteristics holds future promise for both more sophisticated application of existing chemotherapeutic drugs and design of new ones. In particular, the *MYB-NFIB* fusion is an appealing target in that it is highly prevalent in and specific for ACC.(48) Our data implicate that targeting *NFIB* alone may also be of high yield. Rho signaling has already been the subject of research as a target of precision anticancer therapy given its role in many human cancers,(49), and axonal guidance signaling has also been proposed as a viable therapeutic target.(50) These pathways may be worth investigation in the context of ACC.(50)

This whole-genome sequencing study highlights new pathways that may contribute to the carcinogenesis of ACC and suggests novel therapeutic areas that may be relevant to the management of ACC. Importantly, we also confirm observations from several previous sequencing studies. Further research will be required to elucidate the functional significance of our findings, which ultimately may contribute to the development of targeted, effective therapeutics for long-term control of this rare but aggressive disease.

Supplementary Material

Refer to Web version on PubMed Central for supplementary material.

Acknowledgments

We thank our patients for their courage and generosity, and we thank Dr. Srinivasan Yegnasubramanian and the Next Generation Sequencing Center at the Johns Hopkins Sidney Kimmel Comprehensive Cancer Center, supported by NIH grant P30 CA006973, for their support with the high-throughput RNA sequencing experiments.

Financial support: This work was supported by Adenoid Cystic Carcinoma Research Foundation (N. Agrawal, P. Ha), NIH/NIDCR grant DE023218 (N. Agrawal), NIH/NIDCR Specialized Program of Research Excellence grant DE019032 (N. Agrawal), the Virginia and D.K. Ludwig Fund for Cancer Research (N. Agrawal, N. Papadopoulos, K. W. Kinzler, B. Vogelstein), The Sol Goldman Center for Pancreatic Cancer Research (N. Papadopoulos, K. W. Kinzler, B. Vogelstein), NIH/NIDCR R01-DE023227 (P. Ha), and NIH/NIDCR grant T32 DC000027 (E. Rettig).

References

1. Liu J, Shao C, Tan ML, Mu D, Ferris RL, Ha PK. Molecular biology of adenoid cystic carcinoma. Head Neck. 2012; 34:1665–1677. [PubMed: 22006498]
2. Fordice J, Kershaw C, El-Naggar A, Goepfert H. Adenoid cystic carcinoma of the head and neck: predictors of morbidity and mortality. Arch Otolaryngol Head Neck Surg. 1999; 125:149–152. [PubMed: 10037280]
3. Marcinow A, Ozer E, Teknos T, Wei L, Hurtuk A, Old M, et al. Clinicopathologic predictors of recurrence and overall survival in adenoid cystic carcinoma of the head and neck: A single institutional experience at a tertiary care center. Head Neck. 2013
4. Persson M, Andren Y, Mark J, Horlings HM, Persson F, Stenman G. Recurrent fusion of MYB and NFIB transcription factor genes in carcinomas of the breast and head and neck. Proc Natl Acad Sci U S A. 2009; 106:18740–18744. [PubMed: 19841262]
5. Ho AS, Kannan K, Roy DM, Morris LG, Ganly I, Katabi N, et al. The mutational landscape of adenoid cystic carcinoma. Nat Genet. 2013; 45:791–798. [PubMed: 23685749]
6. Stephens PJ, Davies HR, Mitani Y, Van Loo P, Shlien A, Tarpey PS, et al. Whole exome sequencing of adenoid cystic carcinoma. J Clin Invest. 2013; 123:2965–2968. [PubMed: 23778141]
7. Ross JS, Wang K, Rand JV, Sheehan CE, Jennings TA, Al-Rohil RN, et al. Comprehensive genomic profiling of relapsed and metastatic adenoid cystic carcinomas by next-generation sequencing reveals potential new routes to targeted therapies. Am J Surg Pathol. 2014; 38:235–238. [PubMed: 24418857]
8. West RB, Kong C, Clarke N, Gilks T, Lipsick JS, Cao H, et al. MYB expression and translocation in adenoid cystic carcinomas and other salivary gland tumors with clinicopathologic correlation. Am J Surg Pathol. 2011; 35:92–99. [PubMed: 21164292]
9. Mitani Y, Li J, Rao PH, Zhao YJ, Bell D, Lippman SM, et al. Comprehensive analysis of the MYB-NFIB gene fusion in salivary adenoid cystic carcinoma: Incidence, variability, and clinicopathologic significance. Clin Cancer Res. 2010; 16:4722–4731. [PubMed: 20702610]
10. Brill LB 2nd, Kanner WA, Fehr A, Andren Y, Moskaluk CA, Loning T, et al. Analysis of MYB expression and MYB-NFIB gene fusions in adenoid cystic carcinoma and other salivary neoplasms. Mod Pathol. 2011; 24:1169–1176. [PubMed: 21572406]
11. Persson M, Andren Y, Moskaluk CA, Frierson HF Jr, Cooke SL, Futreal PA, et al. Clinically significant copy number alterations and complex rearrangements of MYB and NFIB in head and neck adenoid cystic carcinoma. Genes Chromosomes Cancer. 2012; 51:805–817. [PubMed: 22505352]
12. Mitani Y, Liu B, Rao P, Borra V, Zafereo M, Weber RS, et al. Novel MYBL1 gene rearrangements with recurrent MYBL1-NFIB fusions in salivary adenoid cystic carcinomas lacking t(6;9) translocations. Clin Cancer Res. 2015
13. [accessed December 20, 2015] Phred - Quality Base Calling. Available from URL: http://www.phrap.com/phred/
14. [accessed December 20, 2015] UCSC Genome Bioinformatics. Available from URL: https://genome.ucsc.edu/
15. Hoang ML, Chen CH, Sidorenko VS, He J, Dickman KG, Yun BH, et al. Mutational signature of aristolochic acid exposure as revealed by whole-exome sequencing. Sci Transl Med. 2013; 5:197ra102.
16. Zhang M, Wang Y, Jones S, Sausen M, McMahon K, Sharma R, et al. Somatic mutations of SUZ12 in malignant peripheral nerve sheath tumors. Nat Genet. 2014; 46:1170–1172. [PubMed: 25305755]
17. Jones S, Zhang X, Parsons DW, Lin JC, Leary RJ, Angenendt P, et al. Core signaling pathways in human pancreatic cancers revealed by global genomic analyses. Science. 2008; 321:1801–1806. [PubMed: 18772397]
18. Sausen M, Leary RJ, Jones S, Wu J, Reynolds CP, Liu X, et al. Integrated genomic analyses identify ARID1A and ARID1B alterations in the childhood cancer neuroblastoma. Nat Genet. 2013; 45:12–17. [PubMed: 23202128]

19. Li B, Dewey CN. RSEM: accurate transcript quantification from RNA-Seq data with or without a reference genome. BMC Bioinformatics. 2011; 12:323. [PubMed: 21816040]
20. Kim D, Salzberg SL. TopHat-Fusion: an algorithm for discovery of novel fusion transcripts. Genome Biol. 2011; 12:R72. [PubMed: 21835007]
21. Leng N, Dawson JA, Thomson JA, Ruotti V, Rissman AI, Smits BM, et al. EBSeq: an empirical Bayes hierarchical model for inference in RNA-seq experiments. Bioinformatics. 2013; 29:1035–1043. [PubMed: 23428641]
22. Cancer Genome Atlas N. Comprehensive genomic characterization of head and neck squamous cell carcinomas. Nature. 2015; 517:576–582. [PubMed: 25631445]
23. Law CW, Chen Y, Shi W, Smyth GK. voom: Precision weights unlock linear model analysis tools for RNA-seq read counts. Genome Biol. 2014; 15:R29. [PubMed: 24485249]
24. Ritchie ME, Phipson B, Wu D, Hu Y, Law CW, Shi W, et al. limma powers differential expression analyses for RNA-sequencing and microarray studies. Nucleic Acids Res. 2015; 43:e47. [PubMed: 25605792]
25. Frierson HF Jr, El-Naggar AK, Welsh JB, Sapinoso LM, Su AI, Cheng J, et al. Large scale molecular analysis identifies genes with altered expression in salivary adenoid cystic carcinoma. Am J Pathol. 2002; 161:1315–1323. [PubMed: 12368205]
26. Ramsay RG, Gonda TJ. MYB function in normal and cancer cells. Nat Rev Cancer. 2008; 8:523–534. [PubMed: 18574464]
27. Gao R, Cao C, Zhang M, Lopez MC, Yan Y, Chen Z, et al. A unifying gene signature for adenoid cystic cancer identifies parallel MYB-dependent and MYB-independent therapeutic targets. Oncotarget. 2014; 5:12528–12542. [PubMed: 25587024]
28. Geurts JM, Schoenmakers EF, Roijer E, Astrom AK, Stenman G, van de Ven WJ. Identification of NFIB as recurrent translocation partner gene of HMGIC in pleomorphic adenomas. Oncogene. 1998; 16:865–872. [PubMed: 9484777]
29. Italiano A, Ebran N, Attias R, Chevallier A, Monticelli I, Mainguene C, et al. NFIB rearrangement in superficial, retroperitoneal, and colonic lipomas with aberrations involving chromosome band 9p22. Genes Chromosomes Cancer. 2008; 47:971–977. [PubMed: 18663748]
30. Ramkissoon LA, Horowitz PM, Craig JM, Ramkissoon SH, Rich BE, Schumacher SE, et al. Genomic analysis of diffuse pediatric low-grade gliomas identifies recurrent oncogenic truncating rearrangements in the transcription factor MYBL1. Proc Natl Acad Sci U S A. 2013; 110:8188–8193. [PubMed: 23633565]
31. Brayer KJ, Frerich CA, Kang H, Ness SA. Recurrent Fusions in MYB and MYBL1 Define a Common, Transcription Factor-Driven Oncogenic Pathway in Salivary Gland Adenoid Cystic Carcinoma. Cancer Discov. 2015
32. Iriyama T, Takeda K, Nakamura H, Morimoto Y, Kuroiwa T, Mizukami J, et al. ASK1 and ASK2 differentially regulate the counteracting roles of apoptosis and inflammation in tumorigenesis. EMBO J. 2009; 28:843–853. [PubMed: 19214184]
33. Dooley AL, Winslow MM, Chiang DY, Banerji S, Stransky N, Dayton TL, et al. Nuclear factor I/B is an oncogene in small cell lung cancer. Genes Dev. 2011; 25:1470–1475. [PubMed: 21764851]
34. Moon HG, Hwang KT, Kim JA, Kim HS, Lee MJ, Jung EM, et al. NFIB is a potential target for estrogen receptor-negative breast cancers. Mol Oncol. 2011; 5:538–544. [PubMed: 21925980]
35. Vega FM, Ridley AJ. Rho GTPases in cancer cell biology. FEBS Lett. 2008; 582:2093–2101. [PubMed: 18460342]
36. Parri M, Chiarugi P. Rac and Rho GTPases in cancer cell motility control. Cell Commun Signal. 2010; 8:23. [PubMed: 20822528]
37. Sanz-Moreno V, Gadea G, Ahn J, Paterson H, Marra P, Pinner S, et al. Rac activation and inactivation control plasticity of tumor cell movement. Cell. 2008; 135:510–523. [PubMed: 18984162]
38. Gomez del Pulgar T, Benitah SA, Valeron PF, Espina C, Lacal JC. Rho GTPase expression in tumourigenesis: evidence for a significant link. Bioessays. 2005; 27:602–613. [PubMed: 15892119]

39. Rihet S, Vielh P, Camonis J, Goud B, Chevillard S, de Gunzburg J. Mutation status of genes encoding RhoA, Rac1, and Cdc42 GTPases in a panel of invasive human colorectal and breast tumors. J Cancer Res Clin Oncol. 2001; 127:733–738. [PubMed: 11768613]
40. Gohrig A, Detjen KM, Hilfenhaus G, Korner JL, Welzel M, Arsenic R, et al. Axon guidance factor SLIT2 inhibits neural invasion and metastasis in pancreatic cancer. Cancer Res. 2014; 74:1529–1540. [PubMed: 24448236]
41. Bapat AA, Hostetter G, Von Hoff DD, Han H. Perineural invasion and associated pain in pancreatic cancer. Nat Rev Cancer. 2011; 11:695–707. [PubMed: 21941281]
42. Aster JC, Blacklow SC. Targeting the Notch pathway: twists and turns on the road to rational therapeutics. J Clin Oncol. 2012; 30:2418–2420. [PubMed: 22585704]
43. Agrawal N, Frederick MJ, Pickering CR, Bettegowda C, Chang K, Li RJ, et al. Exome sequencing of head and neck squamous cell carcinoma reveals inactivating mutations in NOTCH1. Science. 2011; 333:1154–1157. [PubMed: 21798897]
44. Rettig EM, Chung CH, Bishop JA, Howard JD, Sharma R, Li RJ, et al. Cleaved NOTCH1 expression pattern in head and neck squamous cell carcinoma is associated with NOTCH1 mutation, HPV status and high-risk features. Cancer Prev Res (Phila). 2015
45. Ranganathan P, Weaver KL, Capobianco AJ. Notch signalling in solid tumours: a little bit of everything but not all the time. Nat Rev Cancer. 2011; 11:338–351. [PubMed: 21508972]
46. Kagawa S, Natsuizaka M, Whelan KA, Facompre N, Naganuma S, Ohashi S, et al. Cellular senescence checkpoint function determines differential Notch1-dependent oncogenic and tumor-suppressor activities. Oncogene. 2014 0.
47. Schwienbacher C, De Grandi A, Fuchsberger C, Facheris MF, Svaldi M, Wjst M, et al. Copy number variation and association over T-cell receptor genes--influence of DNA source. Immunogenetics. 2010; 62:561–567. [PubMed: 20582410]
48. Chae YK, Chung SY, Davis AA, Carneiro BA, Chandra S, Kaplan J, et al. Adenoid cystic carcinoma: current therapy and potential therapeutic advances based on genomic profiling. Oncotarget. 2015
49. Lin Y, Zheng Y. Approaches of targeting Rho GTPases in cancer drug discovery. Expert Opin Drug Discov. 2015; 10:991–1010. [PubMed: 26087073]
50. Gara RK, Kumari S, Ganju A, Yallapu MM, Jaggi M, Chauhan SC. Slit/Robo pathway: a promising therapeutic target for cancer. Drug Discov Today. 2015; 20:156–164. [PubMed: 25245168]

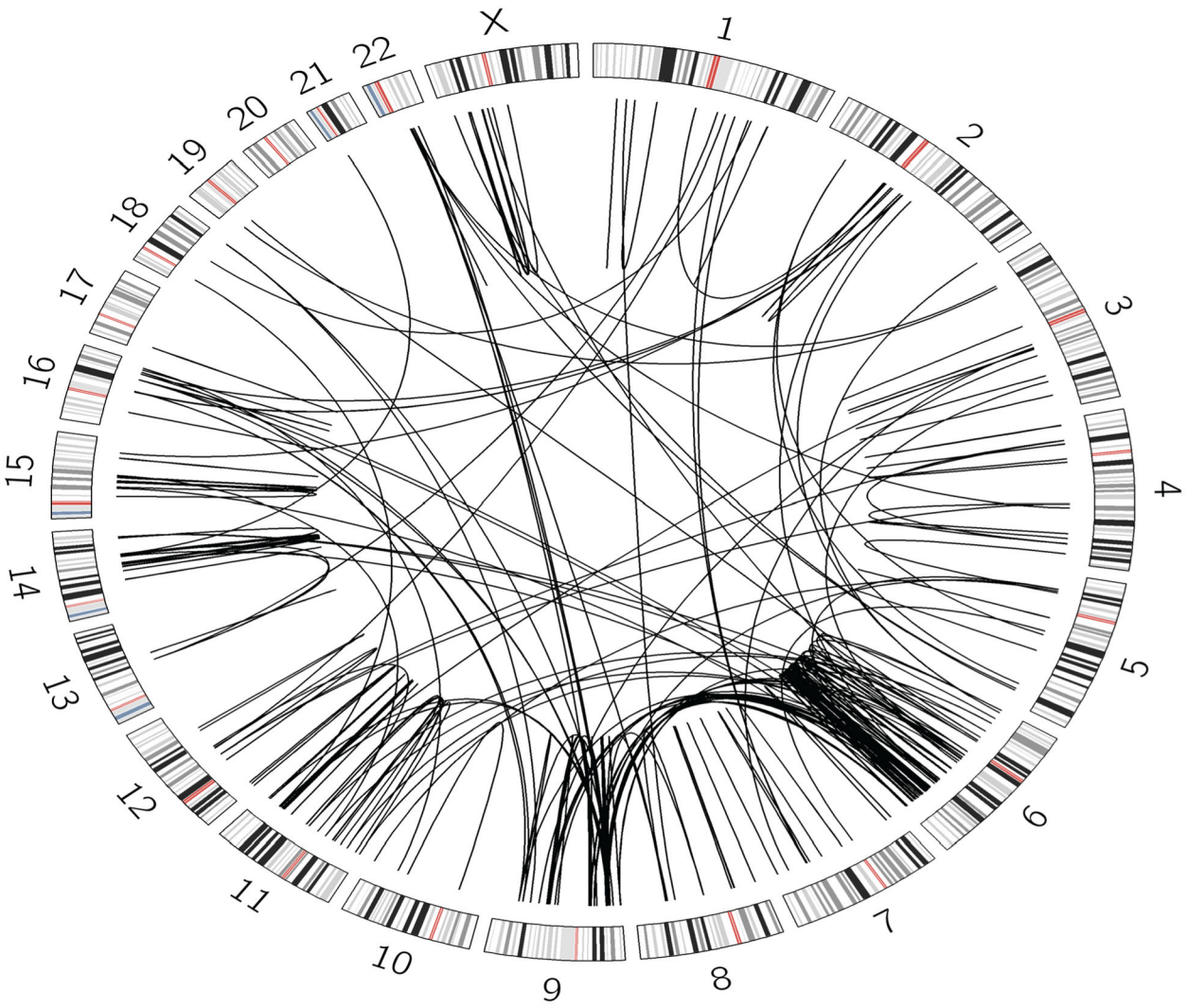

Figure 1.
Chromosomal rearrangements identified in 25 adenoid cystic carcinomas.

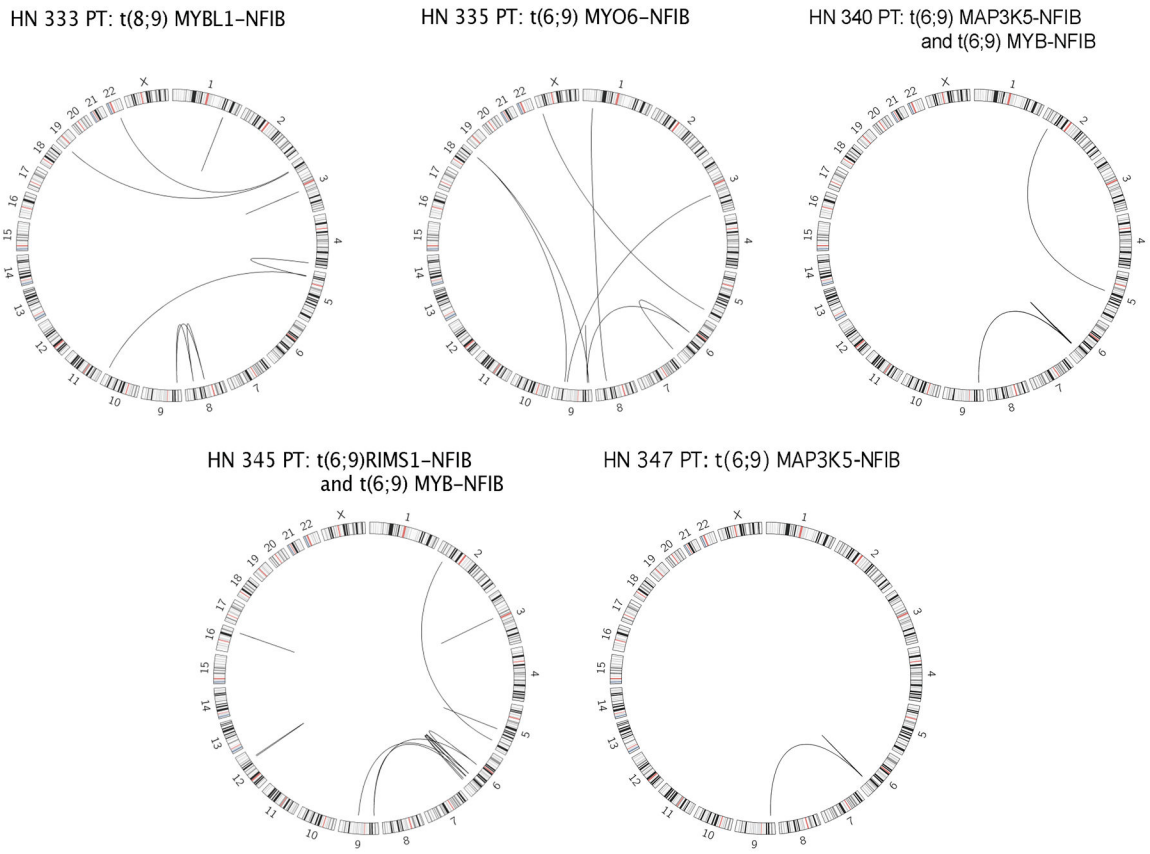

Figure 2.

Circos plots for adenoid cystic carcinomas containing interchromosomal rearrangements in which *NFIB* recombines with gene other than *MYB*.

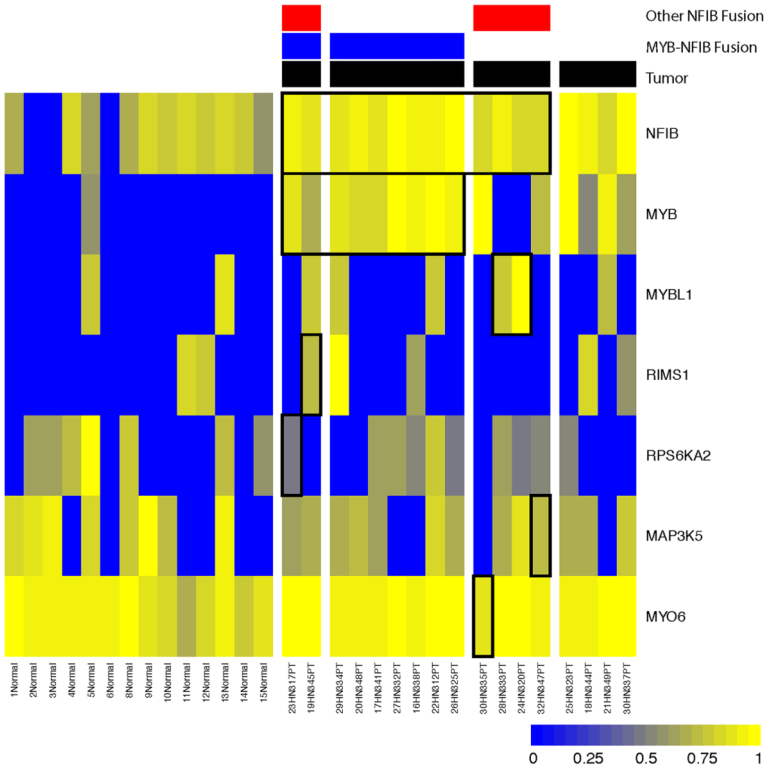

Figure 3.

Heatmap of mRNA expression for genes involved in *NFIB* fusions in ACC tumors compared with normal tissues. Black outline indicates fusion gene DNA transcripts detected on whole-genome sequencing.

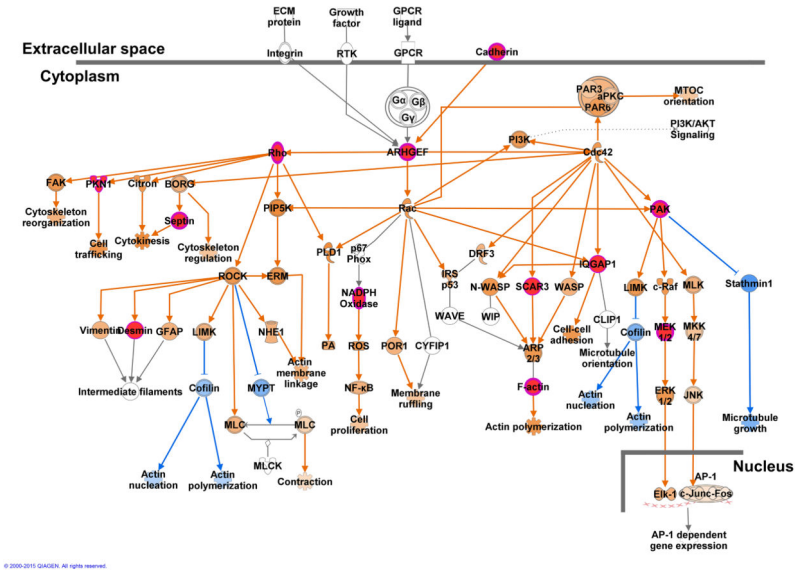

Figure 4 Legend

Molecule Shapes

- Complex/Group
- Chemical/Drug/Toxicant
- Cytokine/Growth Factor
- Other
- G-protein Coupled Receptor
- Ligand-dependent Nuclear Receptor
- Transcription Regulator
- Transmembrane Receptor
- Enzyme
- Function
- Kinase
- Transcription Regulator
- Peptidase

Relationship Types[a]

- A — B: chemical-chemical interactions, chemical-protein interactions, correlation, protein-protein interactions, RNA-RNA interactions: non targeting interactions
- A → B: activation, causation, expression, localization, membership, modification, molecular cleavage, phosphorylation, protein-DNA interactions, protein-RNA interactions, regulation of binding, transcription
- A ⊣ B: inhibition, ubiquitination
- A → B: inhibits and acts on
- direct interaction
- indirect interaction

Color coding: Red/magenta, affected by somatic mutation. Orange, normally activated in pathway affected upstream by somatic mutation. Blue, normally inhibited in pathway affected upstream by somatic mutation. Darker colors indicate higher level of confidence, lighter colors indicate lower level of confidence.

[a]Relationship types: An arrow pointing from A to B signifies different actions for different circumstances. For **signaling pathways**, an arrow pointing from A to B signifies that A causes B to be activated (includes any direct interaction, e.g. binding, phosphorylation, dephosphorylation etc). For **metabolic pathways**, an arrow pointing from A to B signifies that B is produced from A. **For ligands/receptors**, an arrow pointing from a ligand to a receptor signifies that the ligand binds the receptor and subsequently leads to activation of the receptor. This binding event does not necessarily directly activate the receptor; activation of the receptor could be caused by events secondary to the ligand/receptor binding event.

Figure 4.

Rho Family GTPase signaling pathway alterations in adenoid cystic carcinoma.

Table 1

Summary of common genetic alterations in each tumor sample

	Somatic mutations[a]					CNVs			Rearrangements				Tumor Site	
Sample ID	**Number mutations**	***NOTCH1* mutation[b]**	**Chromatin gene mutation[b]**	**Rho family signaling mutation[b]**	**Axonal guidance signaling mutation[b]**	**Number CNVs**	**Tcell receptor gene amplification**	**DUX4 gene deletion**	**Number intrachr.**	**Number interchr.**	**MYB-NFIB translocation[b,c]**	**Other NFIB translocation[c]**	**Major vs. Minor gland**	**Site**
HN 317 PT	14	X					--	-	21	21	**X**	RPS6KA2-NFIB	minor	ethmoid
HN 345 PT	15			X			--	-	8	4	**X**	**RIMS1-NFIB**	minor	maxilla
HN 340 PT	5					3	X	-	2	5	*X*	*MAP3K5-NFIB*	major	parotid
HN 333 PT	23			X	X		-	-	3	6		MYBL1-NFIB	major	submandibular
HN 335 PT	9	X	X			1	-	-	2	6		MYO6-NFIB	major	submandibular
HN 320 PT	6					1	-	-	3	1		**MYBL1-NFIB**	minor	maxillary sinus
HN 347 PT	2						-	-	1	1		*MAP3K5-NFIB*	major	parotid
HN 334 PT	10			X	X		-	-	19	12	**X**		major	parotid
HN 348 PT	22			X			-	-	13	7	**X**		major	submandibular
HN 341 PT	25			X	X	2	X	-	10	3	**X**		minor	maxilla
HN 332 PT	14		X		X	9	-	-	7	1	**X**		major	parotid
HN 350 PT	18			X	X		-	-	4	3	*X*		minor	maxilla
HN 338 PT	33		X	X	X	3	X	-	2	2	**X**		minor	lip
HN 312 PT	28		X	X	X	3	-	X	1	1	**X**		minor	maxillary sinus
HN 325 PT	7					6	-	X		1	**X**		minor	hard palate
HN 343 PT	18		X	X		2	X	-	9	12			minor	septum
HN 324 PT	17		X		X	3	X	-	7	12			major	sublingual gland
HN 318 PT	16		X		X		-	-	8	4			major	parotid
HN 336 PT	11			X			-	-	3	8			minor	ear
HN 308 PT2	8				X	7	X	X	4	2			major	parotid
HN 313 PT	13		X		X		--	-	6				minor	BOT
HN 323 PT	27		X				-	-	1	3			minor	maxillary sinus
HN 344 PT	13		X		X		-	-	1	3			minor	maxilla
HN 349 PT	36	X	X	X	X		-	-					minor	maxilla
HN 337 PT	6				X	1	X	-					minor	palate
Totals	**388**	**3**	**11**	**11**	**14**	**41**	**7**	3	**135**	**118**	**11**	**7**		
Median (IQR) or % of tumors with	14 (9–22)	12%	44%	44%	56%	0 (0–3)	24%	12%	3 (1–8)	3 (1–6)	44%	24%	**10 (40%) major 15 (60%) minor**	

[a] Includes point mutations and small indels.

[b] 'X' indicates tumors with the listed characteristic, '□' indicates lack of the listed characteristic

[c] Bold: mRNA transcript also detected. Italicized: not tested for mRNA.

Abbreviations: CNV, copy number variation; intrachr., intrachromosomal; interchr., interchromosomal; IQR, interquartile range

Table 2

Top mutated genes in adenoid cystic carcinoma[a]

Gene	Number Mutations (N=396)	Number Tumors (N=25)	Gene Size	Mutations/ Mb
NOTCH1	4	3	7668	21
MLL2	3	2	16614	7
ABCA4	2	2	6822	12
COL4A2-AS2	2	2	1062	75
EP300	2	2	7245	11
KANK4	2	2	2988	27
KDM6A	2	2	4227	19
MLL3	2	2	14907	5
PLXNB1	2	2	6408	12
PRKD1	2	2	2763	29
RHOA	2	2	582	137
RP1L1	2	2	7203	11
SF3B1	2	2	3915	20
SKP2	2	2	1275	63
TTN	2	2	100272	1
ZNF292	2	2	8172	10
APOA1	2	1	804	100
BRD1	2	1	3570	22
HBS1L	2	1	2055	39
R3HDM2	2	1	3033	26
SPHKAP	2	1	5103	16

[a]Includes point mutations and small indels. Abbreviations: Mb, megabase.